

A prototype of R-K/200 quantum Hall array resistance standard on epitaxial graphene

A. Lartsev, S. Lara-Avila, A. Danilov, S. Kubatkin, A. Tzalenchuk and Rositsa Yakimova

Linköping University Post Print



N.B.: When citing this work, cite the original article.

Original Publication:

A. Lartsev, S. Lara-Avila, A. Danilov, S. Kubatkin, A. Tzalenchuk and Rositsa Yakimova, A prototype of R-K/200 quantum Hall array resistance standard on epitaxial graphene, 2015, Journal of Applied Physics, (118), 4, 044506.

<http://dx.doi.org/10.1063/1.4927618>

Copyright: American Institute of Physics (AIP)

<http://www.aip.org/>

Postprint available at: Linköping University Electronic Press

<http://urn.kb.se/resolve?urn=urn:nbn:se:liu:diva-120874>

A prototype of RK /200 quantum Hall array resistance standard on epitaxial graphene

A. Lartsev, S. Lara-Avila, A. Danilov, S. Kubatkin, A. Tzalenchuk, and R. Yakimova

Citation: *Journal of Applied Physics* **118**, 044506 (2015); doi: 10.1063/1.4927618

View online: <http://dx.doi.org/10.1063/1.4927618>

View Table of Contents: <http://scitation.aip.org/content/aip/journal/jap/118/4?ver=pdfcov>

Published by the [AIP Publishing](#)

Articles you may be interested in

[Low contact resistance in epitaxial graphene devices for quantum metrology](#)

AIP Advances **5**, 087134 (2015); 10.1063/1.4928653

[Towards a graphene-based quantum impedance standard](#)

Appl. Phys. Lett. **105**, 073511 (2014); 10.1063/1.4893940

[Precision quantum Hall resistance measurement on epitaxial graphene device in low magnetic field](#)

Appl. Phys. Lett. **103**, 173509 (2013); 10.1063/1.4826641

[Observation of the quantum Hall effect in epitaxial graphene on SiC\(0001\) with oxygen adsorption](#)

Appl. Phys. Lett. **100**, 253109 (2012); 10.1063/1.4729824

[Graphene p-n junction arrays as quantum-Hall resistance standards](#)

Appl. Phys. Lett. **99**, 022112 (2011); 10.1063/1.3608157

The new SR865 2 MHz Lock-In Amplifier ... \$7950



SRS Stanford Research Systems
www.thinkSRS.com · Tel: (408)744-9040



Chart recording



FFT displays



Trend analysis

Features

- Intuitive front-panel operation
- Touchscreen data display
- Save data & screen shots to USB flash drive
- Embedded web server and iOS app
- Synch multiple SR865s via 10 MHz timebase I/O
- View results on a TV or monitor (HDMI output)

Specs

- 1 mHz to 2 MHz
- 2.5 nV/√Hz input noise
- 1 μs to 30 ks time constants
- 1.25 MHz data streaming rate
- Sine out with DC offset
- GPIB, RS-232, Ethernet & USB

A prototype of $R_K/200$ quantum Hall array resistance standard on epitaxial graphene

A. Lartsev,¹ S. Lara-Avila,¹ A. Danilov,¹ S. Kubatkin,¹ A. Tzalenchuk,² and R. Yakimova³

¹*Department of Microtechnology and Nanoscience, Chalmers University of Technology, S-41296 Göteborg, Sweden*

²*National Physical Laboratory, Teddington TW110LW, United Kingdom and Royal Holloway, University of London, Egham TW200EX, United Kingdom*

³*Department of Physics, Chemistry and Biology (IFM), Linköping University, S-58183 Linköping, Sweden and Graphensic AB, SE-58330 Linköping, Sweden*

(Received 20 April 2015; accepted 18 July 2015; published online 29 July 2015)

Epitaxial graphene on silicon carbide is a promising material for the next generation of quantum Hall resistance standards. Single Hall bars made of graphene have already surpassed their state-of-the-art GaAs based counterparts as an $R_K/2$ ($R_K = h/e^2$) standard, showing at least the same precision and higher breakdown current density. Compared to single devices, quantum Hall arrays using parallel or series connection of multiple Hall bars can offer resistance values spanning several orders of magnitude and (in case of parallel connection) significantly larger measurement currents, but impose strict requirements on uniformity of the material. To evaluate the quality of the available material, we have fabricated arrays of 100 Hall bars connected in parallel on epitaxial graphene. One out of four devices has shown quantized resistance that matched the correct value of $R_K/200$ within the measurement precision of 10^{-4} at magnetic fields between 7 and 9 T. The defective behaviour of other arrays is attributed mainly to non-uniform doping. This result confirms the acceptable quality of epitaxial graphene, pointing towards the feasibility of well above 90% yield of working Hall bars. © 2015 AIP Publishing LLC. [<http://dx.doi.org/10.1063/1.4927618>]

I. INTRODUCTION

The quantum Hall effect (QHE) provides a primary standard of electrical resistance with a value of a rational fraction of $R_K = h/e^2$.^{1,2} It arises in quasi-2D electron systems as a consequence of Landau quantization in strong magnetic fields. Whenever the Fermi energy lies inside a mobility gap between two Landau levels,³ transversal resistivity becomes equal to R_K/ν , where the filling factor ν is an integer, and longitudinal resistivity vanishes. It has been established that as long as good quantization⁴ is achieved, the value of quantum Hall resistance is universal, that is, does neither depend on the device nor depend on the material within the best available measurement precision.⁵⁻⁷ The ultimate precision, which in the most accurate experiments is on the order of 10^{-10} , is typically set by the signal to noise ratio which, in turn, is limited by the QHE breakdown. The breakdown limits the amount of current that can be passed through the device while preserving the QHE, and it is believed to be caused by overheating of the electron system.⁸

Because of its universality, the QHE is officially used in metrology since 1990 as the representation of the ohm.⁹ The current state-of-the-art quantum Hall resistance standards are based on GaAs/AlGaAs heterostructures, owing to fundamental as well as practical reasons. The low effective mass in GaAs translates to a large separation between the Landau levels, making it easier to avoid thermal occupation of higher levels; also, fabrication of 2DEGs in GaAs heterostructures is a well established technology which reliably yields high quality devices. The observation of QHE in monolayer graphene^{10,11} has opened a new page in metrology, since zero

effective mass and a high Fermi velocity of the charge carriers lead to an even larger Landau level spacing (1300 K at 10 T, compared to 200 K in GaAs), meaning that it can be possible to achieve the same precision at higher temperatures and/or lower magnetic fields. Epitaxial graphene on silicon carbide brings an additional advantage: the breakdown current density can be an order of magnitude higher than the best values achieved in semiconductors,¹² which has been mainly attributed to better thermal coupling between the electron system and the lattice. Better critical current density means that it can be easier to achieve higher critical currents, since the required channel width is then smaller, and the material properties are thus more likely to be uniform across the channel. In a recent direct comparison of quantum Hall resistance between epitaxial graphene and GaAs,¹³ the relative uncertainty of 10^{-10} was limited by the breakdown current in the GaAs device.

Good quantization in the quantum Hall regime is only observed for plateaus with a low filling factor: $\nu = 2$ and possibly $\nu = 4$.¹⁴ Therefore, a single quantum Hall device can provide a standard of resistance with a value $R_K/2 \approx 12.9$ k Ω or $R_K/4 \approx 6.45$ k Ω . In graphene, only the $\nu = 2$ plateau gives a good precision, so that only the $R_K/2$ standard is immediately available. However, by using a combination of series and parallel connections of the Hall bars, it is possible to get a resistance standard with the value of any rational multiple of R_K .^{15,16} The need for values other than $R_K/2$ comes from one of the important tasks in resistance metrology, which is calibration of secondary resistance standards ranging from milliohms to megaohms against a quantum Hall

standard. Having a set of quantum standards with a wide range of values can make this calibration technically easier and more precise. Additionally, a low-resistance quantum standard that uses parallel connection of many Hall bars can exhibit a much larger breakdown current since only a small fraction of the total current flows through every individual Hall bar. For example, $R_K/258.125$ and $R_K/200$ standards based on GaAs¹⁴ tolerated currents up to 4 mA, high enough for a conventional resistance bridge to be used instead of a technically complex cryogenic current comparator for the calibration.

A successful fabrication of a similar device on graphene is expected to provide a resistance standard with an even higher critical current, or, alternatively, a more user-friendly standard operating at a higher temperature and a lower magnetic field. The $\nu=2$ plateau in epitaxial graphene is exceptionally wide¹² due to the pinning of the filling factor caused by interaction with the substrate,¹⁷ which means that small spatial variations in carrier density are less likely to prevent the Hall bars in the array from simultaneously entering a quantum Hall state with a high breakdown current. As a note, similarly wide plateaus with good quantization have recently been reported in graphene produced by chemical vapor deposition on silicon carbide,¹⁸ suggesting that this material is similar to epitaxial graphene, possibly sharing all of its advantages. Additionally, a quantum Hall array requires a relatively complicated design and a large number of lithography steps, so its functional implementation would demonstrate a high reliability of graphene technology. In this work, we report fabrication of a first prototype of a $R_K/200$ standard on epitaxial graphene and discuss its performance.

II. DEVICE DESIGN

In order to be suitable for metrological applications, the quantum Hall array should have relative deviation of resistance from its nominal value within 10^{-8} or less. Although the measurement precision in this work was only 10^{-4} , we took care to eliminate most of the factors that could cause errors on the level of 10^{-8} . To evaluate the effect of different factors, we have simulated an electric circuit corresponding to the array of 100 Hall bars by using Kirchhoff's laws and the relation between the voltage drop over two neighbouring leads of a QHE device and the current through one of them: $V_{m+1} - V_m = R_H I_m$,¹⁹ taking into account the device geometry and, where necessary, a random distribution of various defects.

One important source of deviations are finite (and generally different) contact resistances in the Hall bar structures and resistances of the interconnects, but these deviations can be significantly reduced by a proper circuit design. If the multiple-connection technique^{15,16} is used, the relative deviation of the Hall resistance R from its ideal value R_H/N is $\delta R = N \times R/R_H - 1 = O((R_C/R_H)^K)$, where N is the number of Hall bars, $R_H = R_K/2 \approx 13 \text{ k}\Omega$ is Hall resistance of a single bar, R_C is the typical connection resistance, and K is the number of contact pairs used in each Hall bar. We have chosen quadruple connection ($K=4$) so that this

deviation can be within 10^{-8} for $R_C \sim 100 \Omega$, which is also confirmed by numeric simulations.

Another possible source of error are defects in individual devices coming from the morphology of the material. Epitaxial graphene is never completely monolayer over a large area, but usually has significant inclusions of bilayer.^{20,21} When the monolayer is in the quantum Hall state, these bilayer areas usually form metallic regions.²² According to the general theory, such features do not affect the QHE as long as the area outside these regions is a connected space.³ On the other hand, if a patch of bilayer crosses a Hall bar completely, this will break down the QHE.^{23,24} For example, if a continuous region of bilayer runs along the Hall bar, connecting two current leads (Figure 1(a)) then, assuming metallic behaviour of the bilayer, we predict that this structure will be equivalent to two Hall bars connected as shown in Figure 1(b), which (ignoring resistance of the bilayer connection) gives Hall resistance of $2R_H/3$ instead of R_H . Such 30% deviation in Hall resistance of a single Hall bar will translate to a 100 times smaller 3×10^{-3} deviation for the net resistance of an array of 100 Hall bars. If a patch of bilayer connects two opposite sides of the Hall bar as in Figure 1(c), this will be equivalent to series connection of two Hall bars²² (Figure 1(d)), which introduces an additional longitudinal resistance close to R_H . According to our numeric simulations, one such defect in an array of 100 Hall bars will cause a 10^{-5} relative deviation in resistance, and two defects can cause a deviation of 10^{-4} . Fortunately, on some substrates, the bilayer patches form a sparse set of short stripes, all oriented along the terraces (Figure 2(d)). If a rectangle-shaped Hall bar is also oriented along the terraces, and the length of the Hall bar exceeds that of the patches, this will ensure that the abovementioned problems will not be encountered. One problem that still can occur in a design shown in Figure 2(d) is that a patch of bilayer can connect two contacts on the same side, as in Figure 1(e). However, numeric simulations show that since the potential difference between the affected contacts is small, even 20 randomly placed defects of this type will only cause 1×10^{-5} relative deviation in the net resistance of the array, which is below our measurement precision of 10^{-4} . On the other hand, if

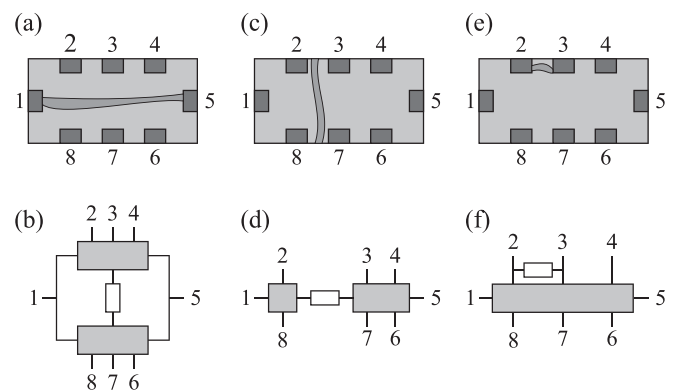


FIG. 1. Defects related to bilayer patches. (a) and (b) A Hall bar with a bilayer region along the channel and its equivalent circuit. (c) and (d) A Hall bar with a bilayer region across the channel and its equivalent circuit. (e) and (f) A Hall bar with a bilayer region at the side and its equivalent circuit.

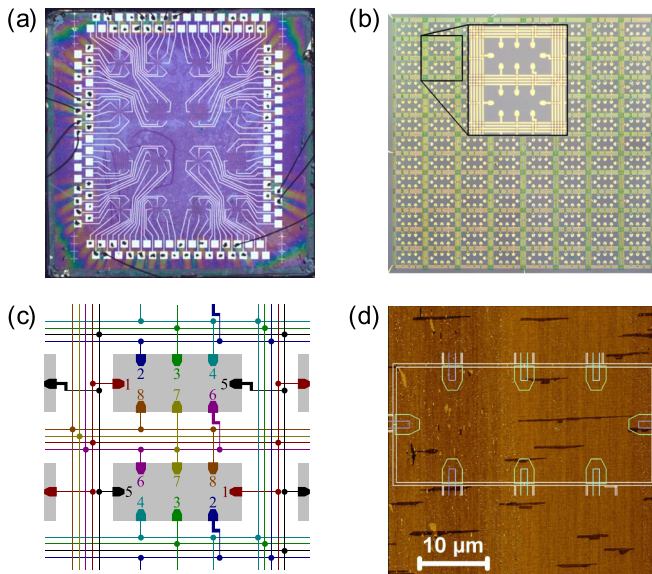


FIG. 2. (a) A microphotograph of the entire chip. (b) A microphotograph of an array of 100 Hall bars. (c) A part of the schematics of the array. The interconnecting wires are arranged with a significant redundancy. (d) A typical AFM phase image of the graphene substrate with the drawing of a Hall bar on top of it. Dark areas are the bilayer patches.

metrological precision is to be reached, this problem must be avoided, for example, by increasing the size of the Hall bars and slightly rotating them with respect to the patches. An even better optimized procedure for graphene growth yielding smaller patches would further reduce the chances of encountering bilayer-related defects.

The devices were fabricated on a substrate²⁵ where the bilayer patches were up to $20 \mu\text{m}$ long. The Hall bars were $40 \times 20 \mu\text{m}$ in size, with the long side oriented along the patches, as shown in Figure 2(d). The Hall bars were kept as small as possible while still larger than the patches in order to reduce the size of the array, as it was not certain that the carrier density in graphene would be uniform over a large area. Small variations in carrier density in individual Hall bars will not affect the array due to the huge width of the $\nu = 2$ plateau,¹⁷ because all Hall bars will be in the quantum Hall state at a strong enough magnetic field. However, if the current density varies over different array elements so much that some elements will not completely enter the quantum Hall regime, the effect on the net resistance could be intolerable. Indeed, even if just one out of 100 Hall bars in the array has Hall resistance $R_{XY} = R_H(1 + \delta R_1)$, which is different from R_H due to not being in a fully developed quantum Hall state, the relative deviation in the resistance of the array caused by this will be $\delta R_1/100$, which for a large enough δR_1 will be noticeable. Finite longitudinal resistivity ρ_{XX} will affect R_{XY} in the array as well:²⁶ the corresponding relative deviation is $O(\rho_{XX}R_C/R_H^2)$ for voltage probes that are directly opposite to each other and $O(\rho_{XX}/R_H)$ for those which are not. Although in our design the voltage probes that are least affected by finite connection resistances alone (4 and 8 or 2 and 6, depending on the direction of the magnetic field) are not opposite to each other and thus do not minimize the effect of longitudinal resistivity, this can be corrected by increasing the length of the Hall bars. As a final

note, reducing the size of the array has an additional advantage that it allows fabricating several devices on a single chip, which is important due to the limited availability of substrates with high quality graphene.

The interconnecting wires were $1 \mu\text{m}$ wide and up to $500 \mu\text{m}$ long. The resistance of the wires was measured to be up to $0.2 \Omega/\mu\text{m}$, and the typical contact resistance was found to be less than 10Ω , so that the connection resistance was expected to be on the level of 100Ω , small enough that its effect on the resistance of the array can be within 10^{-8} . One more possible source of error is the leakage of the insulation between the intersecting wires. We define the insulation resistance R_I as the resistance of the insulation between the system of wires that connects together, for example, contact number 1 in all Hall bars and the system of wires that connects contact number 5 in all Hall bars. We expect that this resistance is similar for all pairs of contacts, and that its relative contribution to the resistance of the array is on the level of $(R_H/N)/R_I$. In order to measure R_I directly, a structure identical to the array of 100 Hall bars was fabricated on a silicon chip covered with 200 nm of silicon oxide. Resistance between two terminals of this device was measured to be $150 \text{ G}\Omega$ at room temperature (Figure 3), which we assume as a lower-bound estimate for R_I . Therefore, the relative contribution of the leakage to the resistance of the array of 100 Hall bars was expected to be on the order of $(R_K/200)/R_I \sim 10^{-9}$ at most. In fact, the effect of the leakage at low temperatures should be even smaller.

III. DEVICE FABRICATION

The devices were fabricated by electron beam lithography in six steps. The first step was used to deposit alignment marks. The contacts (5 nm Ti , 50 nm Au) were deposited in the next step, preventing the graphene/metal interface from possible contamination from the subsequent steps. Then, graphene was patterned by oxygen plasma etching to define the Hall bars and make trenches that would separate the metal wires. Two layers of metal wires connecting the Hall bars, which needed to intersect without electrical contact, were deposited in the subsequent steps: the first layer (5 nm Ti , 50 nm Au), followed by insulation ($100 \text{ nm silicon oxide}$,

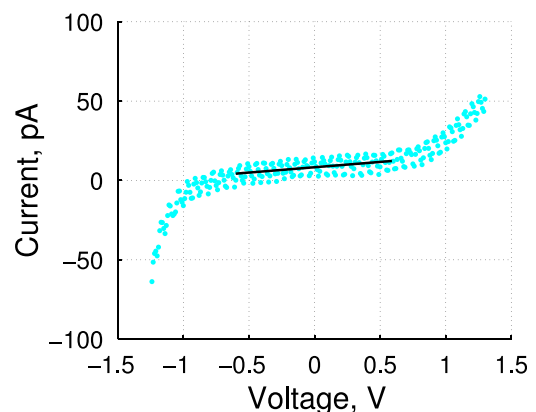


FIG. 3. Measurement of the leakage current between the interconnecting wires of the quantum Hall array. The line represents a linear fit at low voltages, which gives the resistance of $150 \text{ G}\Omega$.

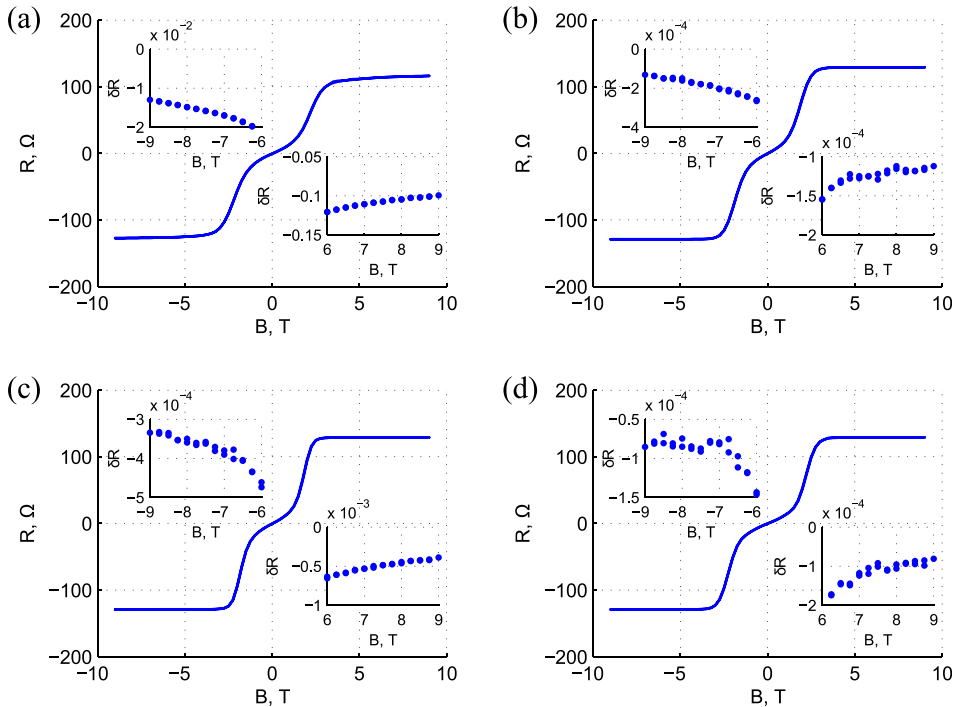


FIG. 4. Measurements of R_{XY} vs. magnetic field on arrays of Hall bars. (a)-(d) correspond to devices A-D. Insets show deviation from the ideal value $R_K/200$, $\delta R = 200 \times R/R_K - 1$ for $B > 0$ and $-200 \times R/R_K$ for $B < 0$, at high fields where the quantum Hall plateaus were expected to be fully developed. The only plateau that is actually fully developed is the one for device D at negative fields.

electron beam deposition), followed by the second layer (5 nm Ti, 150 nm Au). Finally, the devices were spin-coated with 100 nm of P(MMA-MAA) and 300 nm of ZEP for photochemical gating.²⁷ All deposition was made by lift-off technique, so that P(MMA-MAA) e-beam resist and solvents (acetone and the mixture of isopropanol and water) were the only substances the graphene has been in contact with. In total, 16 devices were fabricated on a 7×7 mm chip: single Hall bars and arrays of 4, 16, 36, and 100 Hall bars connected in parallel.

IV. MEASUREMENT DETAILS

Measurements of the quantum Hall resistance were performed at a base temperature of 2 K. Before the measurement, photochemical gating²⁷ was used to reduce the carrier density from $3 \times 10^{12} \text{ cm}^{-2}$ to $4 \times 10^{11} \text{ cm}^{-2}$, as confirmed by Hall measurements at low fields. For the arrays, the Hall voltage V_{XY} was measured between contacts 3 and 7. The theory¹⁵ suggests that the relative correction to R_{XY} due to the finite resistance of the interconnects would then be $O((R_C/R_H)^2) \sim (100 \Omega / 12.9 \text{ k}\Omega)^2 \sim 10^{-4}$. However, our numeric simulations show that due to the particular arrangement of redundant interconnecting wires, this correction is only 10^{-6} for our choice of voltage probes, and this is well below our measurement precision. The advantage of using this pair of voltage probes is that the above stated precision is the same for both directions of magnetic field, and also the effect of finite longitudinal resistance is minimized since the probes are directly opposite to each other and far away from the hot spots at the source and drain contacts.

When several devices were measured at the same time, they were connected in series so that a single current could be used for the excitation. To exclude the effect of thermal voltages and other possible sources of voltage offset, R_{XY} was measured as an average value for two opposite directions of

the current. 100 μA excitation current was used for arrays of 100 Hall bars and 1 μA current for single Hall bars.²⁸

V. MEASUREMENTS OF THE QUANTUM HALL RESISTANCE

Quantized Hall resistance was measured in four arrays of 100 Hall bars (devices A, B, C, and D) in magnetic fields up to 9 T. The four devices showed different relative deviations of R_{XY} from the ideal value of $R_K/200 \approx 129.064 \Omega$, which are shown in Figure 4 and summarized in Table I. Device A was clearly defective, with 10% deviation of R_{XY} for positive field and 1% for negative field. Devices B and C performed better, showing deviations on the level of 1×10^{-4} and 4×10^{-4} , respectively, but the plateaus were not fully developed for any direction of the magnetic field. Device D performed the best: it showed a well defined plateau with a relative deviation of 8×10^{-5} from the ideal value above 7 T for negative fields, and the deviation in R_{XY} was approaching the same value at the maximum positive field. The deviation for device D in negative fields can be explained by the imprecision of the current source and the voltmeter; thus, we assume that one out of four arrays has performed correctly within the available measurement precision.

A hint at the possible reason for the defective behaviour of arrays A-C, as well as of array D at positive fields, is

TABLE I. Relative deviations between the measured Hall resistance of the four arrays and the ideal value $R_K/200$ at the highest magnetic fields.

Device	$-200 \times R/R_K - 1, B < 0$	$200 \times R/R_K - 1, B > 0$
A	-1.3×10^{-2}	-0.1
B	-1.5×10^{-4}	-1.1×10^{-4}
C	-3.3×10^{-4}	-4×10^{-4}
D	-8×10^{-5}	-9×10^{-5}

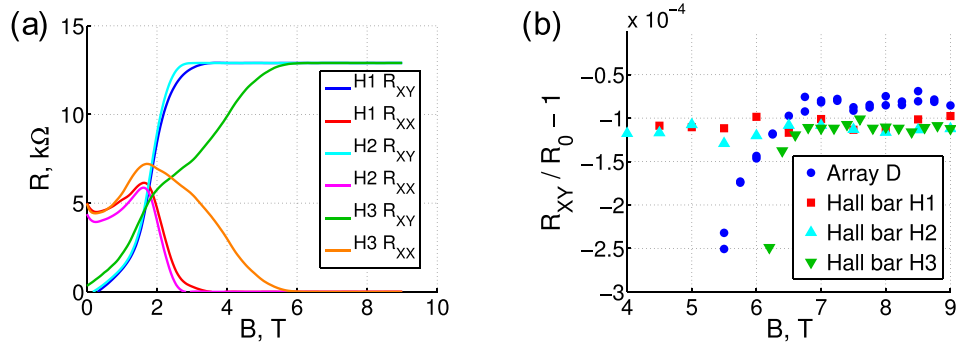


FIG. 5. (a) R_{XY} and R_{XX} as a function of magnetic field in three single Hall bars: H1, H2, and H3. Measurements at negative fields were not performed, since it was sufficient to achieve good quantization for one direction of the field. (b) Relative deviation of R_{XY} for the array D and three Hall bars at the strongest fields (positive fields for the Hall bars, negative fields for the array). $R_0 = R_K/2$ for single Hall bars and $-R_K/200$ for the array. The discrepancy between the single Hall bars and the array is attributed to the imprecision of the voltmeter.

provided by measurements on single Hall bars that were fabricated on the same chip. As seen in Figures 5(a) and 5(b), R_{XY} in the array D as well as in Hall bars H1 and H2 reaches 1% precision around 3 T. The Hall bars H1 and H2 go on to reach the best observed precision at 4 or 4.5 T, which we assume to be the normal behaviour of the material at this carrier density. However, the array D reaches its best precision only at 7 T (Figure 5(b)). That could happen if a few Hall bars in the array had a plateau starting at higher fields due to non-uniform doping, similar to what was observed in the device H3. A similar but more severe problem could be a possible reason for the observed behaviour of arrays B and C, which did not show fully developed plateaus up to 9 T. This non-uniform doping could be either introduced during the graphene growth or caused by the photochemical gating. If the latter is the case, the problem can possibly be avoided by using other methods of controlling the carrier density, such as doping by exposure to different environments^{18,29,30} or gating by corona discharge.³¹

VI. CONCLUSION

We have fabricated a prototype of $R_K/200$ quantum Hall array resistance standard on epitaxial graphene. One out of four devices has shown a fully developed plateau with a correct value of Hall resistance within the measurement precision of 10^{-4} . This confirms that all 100 Hall bars were on a quantum Hall plateau at the same time, and the Hall resistance in each individual Hall bar deviated from the ideal value $R_K/2$ by no more than 1%. We speculate that the defective behaviour of other arrays is caused by non-uniform doping, which may be possible to avoid by using other techniques of carrier density control, such as environmental doping and gating by corona discharge. Our results suggest that large-scale integration of quantum Hall devices on epitaxial graphene is feasible, and we expect that this work will pave the way to a new generation of quantum resistance standards operating at higher temperature, lower magnetic fields, and high currents.

ACKNOWLEDGMENTS

This work was partly supported by EU FP7 STREP ConceptGraphene, the EMRP project GraphOhm, the

Graphene Flagship (Contract No. CNECT-ICT-604391), Swedish Foundation for Strategic Research (SSF), Linnaeus Centre for Quantum Engineering, Knut and Alice Wallenberg Foundation, and Chalmers AoA Nano. The EMRP is jointly funded by the EMRP participating countries within EURAMET and the European Union.

- ¹K. von Klitzing and G. Ebert, *Metrologia* **21**, 11 (1985).
- ²B. Jeckelmann and B. Jeanneret, *Rep. Prog. Phys.* **64**, 1603 (2001).
- ³R. Joynt and R. Prange, *Phys. Rev. B* **29**, 3303 (1984).
- ⁴F. Delahaye and B. Jeckelmann, *Metrologia* **40**, 217 (2003).
- ⁵B. Jeckelmann, B. Jeanneret, and D. Inglis, *Phys. Rev. B* **55**, 13124 (1997).
- ⁶A. Hartland, K. Jones, J. Williams, B. Gallagher, and T. Galloway, *Phys. Rev. Lett.* **66**, 969 (1991).
- ⁷F. Delahaye, D. Dominguez, F. Alexandre, J. Andre, J. Hirtz, and M. Razeghi, *Metrologia* **22**, 103 (1986).
- ⁸S. Komiyama and Y. Kawaguchi, *Phys. Rev. B* **61**, 2014 (2000).
- ⁹P. J. Mohr and B. N. Taylor, *J. Phys. Chem. Ref. Data* **28**, 1713 (1999).
- ¹⁰K. Novoselov, A. K. Geim, S. Morozov, D. Jiang, M. Katsnelson, I. Grigorieva, S. Dubonos, and A. Firsov, *Nature* **438**, 197 (2005).
- ¹¹Y. Zhang, Y.-W. Tan, H. L. Stormer, and P. Kim, *Nature* **438**, 201 (2005).
- ¹²J. Alexander-Webber, A. Baker, T. Janssen, A. Tzalenchuk, S. Lara-Avila, S. Kubatkin, R. Yakimova, B. Piot, D. Maude, and R. Nicholas, *Phys. Rev. Lett.* **111**, 096601 (2013).
- ¹³T. Janssen, J. Williams, N. Fletcher, R. Goebel, A. Tzalenchuk, R. Yakimova, S. Lara-Avila, S. Kubatkin, and V. Fal'ko, *Metrologia* **49**, 294 (2012).
- ¹⁴W. Poirier, A. Bounouh, K. Hayashi, H. Fhima, F. Piquemal, G. Genevès, and J. André, *J. Appl. Phys.* **92**, 2844 (2002).
- ¹⁵F. Delahaye, *J. Appl. Phys.* **73**, 7914 (1993).
- ¹⁶M. Ortolano, M. Abrate, and L. Callegaro, *Metrologia* **52**, 31 (2015).
- ¹⁷T. Janssen, A. Tzalenchuk, R. Yakimova, S. Kubatkin, S. Lara-Avila, S. Kopylov, and V. Fal'ko, *Phys. Rev. B* **83**, 233402 (2011).
- ¹⁸F. Lafont, R. Ribeiro-Palau, D. Kazazis, A. Michon, O. Couturaud, C. Consejo, T. Chassagne, M. Zielinski, M. Portail, B. Jouault *et al.*, *Nat. Commun.* **6**, 6806 (2015); e-print arXiv:1407.3615v2.
- ¹⁹F. Fang and P. Stiles, *Phys. Rev. B* **29**, 3749 (1984).
- ²⁰J. Hass, W. De Heer, and E. Conrad, *J. Phys.: Condens. Matter* **20**, 323202 (2008).
- ²¹R. Yakimova, T. Iakimov, G. Yazdi, C. Bouhafs, J. Eriksson, A. Zakharov, A. Boosalis, M. Schubert, and V. Darakchieva, *Physica B: Condens. Matter* **439**, 54 (2014).
- ²²C. Chua, M. Connolly, A. Lartsev, T. Yager, S. Lara-Avila, S. Kubatkin, S. Kopylov, V. Fal'ko, R. Yakimova, R. Pearce *et al.*, *Nano Lett.* **14**, 3369 (2014).
- ²³T. Löfwander, P. San-Jose, and E. Prada, *Phys. Rev. B* **87**, 205429 (2013).
- ²⁴T. Yager, A. Lartsev, S. Mahashabde, S. Charpentier, D. Davidovikj, A. Danilov, R. Yakimova, V. Panchal, O. Kazakova, A. Tzalenchuk *et al.*, *Nano Lett.* **13**, 4217 (2013).
- ²⁵Supplied by Graphensic AB, <http://graphensic.com>.

- ²⁶W. Poirier, A. Bounouh, F. Piquemal, and J. André, *Metrologia* **41**, 285 (2004).
- ²⁷S. Lara-Avila, K. Moth-Poulsen, R. Yakimova, T. Bjørnholm, V. Fal'ko, A. Tzalenchuk, and S. Kubatkin, *Adv. Mater.* **23**, 878 (2011).
- ²⁸The ratio of the excitation currents has been measured separately and found to be 100.016, thus we assumed 0.99984 μA current for single Hall bars.
- ²⁹Y. Yang, L.-I. Huang, Y. Fukuyama, F.-H. Liu, M. A. Real, P. Barbara, C.-T. Liang, D. B. Newell, and R. E. Elmquist, *Small* **11**, 90 (2015).
- ³⁰T. Yager, M. J. Webb, H. Grennberg, R. Yakimova, S. Lara-Avila, and S. Kubatkin, *Appl. Phys. Lett.* **106**, 063503 (2015).
- ³¹A. Lartsev, T. Yager, T. Bergsten, A. Tzalenchuk, T. M. Janssen, R. Yakimova, S. Lara-Avila, and S. Kubatkin, *Appl. Phys. Lett.* **105**, 063106 (2014).